Construction and validation of an m6A RNA methylation regulator prognostic model for early-stage clear cell renal cell carcinoma

ZHAN WANG[1], MINGXIN ZHANG[2], SAMUEL SEERY[3,4], GUOYANG ZHENG[1], WENDA WANG[1], YANG ZHAO[1], XU WANG[1] and YUSHI ZHANG[1]

[1]Department of Urology, Peking Union Medical College Hospital, Chinese Academy of Medical Science and Peking Union Medical College, Beijing 100730; [2]Department of Urology, The Affiliated Hospital of Qingdao University, Qingdao, Shandong 266003; [3]School of Humanities and Social Sciences, Chinese Academy of Medical Sciences and Peking Union Medical College, Beijing 100730, P.R. China; [4]Faculty of Health and Medicine, Division of Health Research, Lancaster University, Lancaster LA1 4YW, United Kingdom

Received April 2, 2022; Accepted May 27, 2022

DOI: 10.3892/ol.2022.13370

Abstract. N6-methyladenosine (m6A) is the most common type of RNA methylation and is considered to participate in various biological and pathological processes, specifically in the regulation of tumorigenesis and metastasis. However, the exact prognostic role of m6A methylation regulators in early-stage clear cell renal cell carcinoma (ccRCC) is currently unknown. In the present study, a prognostic model consisting of m6A RNA methylation regulators in early stage ccRCC was constructed and the reliability of the signature was assessed by proteomics and immunohistochemistry. Additionally, the relationship between the prognostic model and tumor infiltrating immune cells within the tumor microenvironment was investigated. Gene mutation and RNA sequencing data of 19 m6A methylation regulators for early-stage ccRCC patients were extracted from The Cancer Genome Atlas (TCGA) database with the corresponding clinical information. Univariate and multivariate Cox regression analysis were applied to construct a prognostic model and the proteomic data as well as immunohistochemistry were used to validate the result. The correlations between the prognostic model and tumor infiltrating immune cells were assessed using Spearman's rank correlation analysis. A total of 192 early stage ccRCC gene mutation data as well as 261 RNA sequencing data with relative clinical data were extracted from the TCGA. The overall mutation frequency of the 19 m6A RNA methylation regulators was relatively low with 4.69%. The transcriptome data revealed that 11 genes were differentially expressed between cancer tissues and relatively normal tissues. Survival analysis highlighted four specific genes as having a significant influence on overall survival. An established model with four genes demonstrated the best predictability for early-stage ccRCC. After integrating clinical characteristics into the multivariate analysis, the model remained effective at predicting ccRCC prognosis. Spearman's rank analysis suggested several tumor infiltrating immune cells such as dendric cells, $CD4^+$ cells, $CD8^+$ T cells and macrophages were significantly correlated with the model. Proteomic data analysis as well as immunohistochemistry from the Human Protein Atlas showed that all the genes used to construct the model were differentially expressed between ccRCC and normal tissues. In conclusion, a novel m6A methylation regulators-based prognostic signature was established and validated with proteomics and immunohistochemistry. In addition, the model was significantly correlated with multiple infiltrating immune cells in tumor microenvironment.

Correspondence to: Dr Yushi Zhang, Department of Urology, Peking Union Medical College Hospital, Chinese Academy of Medical Science and Peking Union Medical College, 1 Shuaifuyuan Wangfujing, Dongcheng, Beijing 100730, P.R. China
E-mail: beijingzhangyushi@126.com

Key words: early-stage renal cell carcinoma, clear cell renal cell carcinoma, prognostic model, N6-methyladenosine methylation regulators, proteomics, bioinformatic analysis

Introduction

Renal cell carcinoma (RCC) is one of the most common malignant tumors in urinary system, third only to prostate cancer and bladder cancer (1). According to the latest survey, there were ~76,000 new cases in the United States, including 48,780 men and 27,300 women, which accounts for 3-5% of all malignant tumors (1,2). Prognosis for RCC is relatively favorable when identified at an early stage with five-year survival rates for localized and locally advanced RCC ranging from 70-90% (1). However, once distant metastasis takes place, the five-year survival rate decreases dramatically and can be as little as 10% (1). It is therefore necessary to investigate all possible methods to stratify the RCC patients upon disease initiation and make more individualized follow-up strategies. Clear cell renal cell carcinoma (ccRCC) is the most common

pathological type and accounts for between 60-80% of all types (3). With radiographic imaging becoming common place in routine diagnostics, a dramatic rise in the number of small and early-stage ccRCC cases has also been observed. Tumor, Node, Metastasis (TNM) staging system remains the most commonly used method for determining prognosis of ccRCC. However, for early-stage RCC, the TNM staging system alone is insufficient to determine postoperative treatment and survival prognostics due to its lack of sensitivity and specificity (4). According to the NCCN clinical practice guidelines, for stage I and II RCC, post-operative surveillance is recommended (5). However, if postoperative surveillance or treatment could be more precise for ccRCC patients, the clinical outcomes could be more favorable. That's the reason why certain other staging systems, such as the UISS, Kattan, Yaycioglu and Cindolo model, are being explored and investigated in clinical research (4). It remains of the utmost importance to construct and validate a prognostic model for early-stage RCC.

Recently, accumulating evidence has suggested that as the most common type of RNA modification, N6-methyladenosine (m6A) affects tumorigenesis in various types of cancers and could even hold a function in regulating the tumor immune microenvironment (6-10). In addition, they could also serve as diagnostic and prognostic biomarkers (11). Thus, the gene mutation data and transcriptional sequencing data of The Cancer Genome Atlas (TCGA) database as well as immunohistochemistry staining were combined with our proteomic data detected by high-performance liquid chromatography-mass spectrometry (HPLC-MS) to construct a prognostic model consisting of m6A methylation regulators for early-stage RCC. The relationship between the model and tumor infiltrating immune cells was evaluated, so as to preciously stratify the ccRCC patients and provide new ideas for the inner mechanism related to RCC.

Materials and methods

Data collection and analyzation of 19 m6A methylation regulators from the TCGA database. The gene mutation files and RNA sequencing data (count value) with the corresponding clinical information from ccRCC patients were downloaded from TCGA database (https://portal.gdc.cancer.gov/repository). Based on the clinical data, the 192 somatic mutation data and 261 RNA transcriptomes with early-stage ccRCC (pT1) were selected for inclusion. Data with VarScan2 analysis of somatic mutation and tumor mutation burden were downloaded from TCGA database. The result was displayed with the R packages 'maftools' (12). RNA sequencing counts in tumor tissues and adjacent relatively normal tissues were standardized and analyzed using the DESeq2 package (13).

Proteomic examination of 27 paired early-stage ccRCC tissues. To assess the reliability of the m6A methylation regulator expression across protein levels, 27 paired early-stage ccRCC tissues were then collected and analyzed by means of HPLC-MS. The present study was approved (approval no. KS2021034) by the Institutional Review Board of Peking Union Medical College Hospital, Chinese Academy of Medical Science and Peking Union Medical College (Beijing, China). Formal written consent was requested and signed by all patients to signify approval to participate. All patients received the partial or radical nephrectomy during the period of June 2019 to September 2019 and the ccRCC diagnosis was determined by at least two independent specialists for pathological analysis in our center. The HPLC-MS process was divided into the following steps:

i) Sample collection and preparation: A total of 27 paired ccRCC tissues, including 27 paired tumor and non-cancerous normal tissues (NATs), were collected for further analysis. The ccRCC tissues were resected from the center of the tumor without necrotic regions. NATs were defined as tissues at least 5 mm away from the cancer capsule and no tumor invasion was identified under microscopy. All tissue samples were collected from the operation room and transferred directly into the -80˚C refrigerator for storage until final analysis took place.

A total of ~25-120 mg of each cryo-pulverized renal tumor tissue or NATs were homogenized separately in an appropriate volume of lysis buffer [i.e. 2% SDS, 20 mM Tris, Cocktail (1:100), DNAse (1:100), RNAse (1:1,000)] by repeated vortexing. Protein concentration was determined using Pierce™ BCA assay protein assay kit (Thermo Fisher Scientific, Inc.). A total of 100 mg of protein was reduced with 20 mM dithiothreitol (DTT) for 5 min at 95˚C and subsequently alkylated with 50 mM iodoacetamide for 45 min at room temperature in the dark. Protein digestion was carried out using a filter-aided sample preparation technique method. Proteins were loaded onto 30-kDa filter devices (Pall Life Sciences). Trypsin (Trypsin Gold, mass spec grade, Promega Corporation) was added at an enzyme to protein ratio of 1:50, and samples were incubated at 37˚C overnight.

ii) ESI-LC-MS/MS for proteome library generation: The pooled peptide samples (30 μl) of each group were separated by high-pH RPLC columns (4.6x250 mm, C18, 3 μm; Waters Corporation). Each pooled sample was loaded onto a column in buffer A1 ('H_2O', pH 10). The elution gradient was between 5-30% buffer B1 (90% ACN, pH 10; flow rate, 1 ml/min) for 30 min. Eluted peptides were collected at one fraction per min. After lyophilization, 30 fractions were resuspended in 0.1% formic acid, before being concatenated into 10 fractions by combining fractions 1, 11, 21 and so forth.

In order to generate a spectral library, fractions from RPLC were analyzed in the DDA mode. Parameters were set as follows: the MS was recorded at 350-1,500 m/z at a resolution of 60,000 m/z; the maximum injection time was 50 ms, the auto gain control (AGC) was 1e6, and the cycle time was 3 sec. MS/MS scans were performed at a resolution of 15,000 with an isolation window of 1.6 Da and a collision energy at 32% (HCD); the AGC target was 50,000, and the maximum injection time was 30 ms.

iii) ESI-LC-MS/MS for proteome data-independent acquisition analysis: Digested peptides were dissolved in 0.1% formic acid and separated on an RP C18 self-packing capillary LC column (75 μm x 150 mm, 3 μm). The eluted gradient was 5-30% buffer B2 (0.1% formic acid, 99.9% ACN; flow rate, 0.3 μl/min) for 60 min. For MS acquisition, the

variable isolation window DIA method with 38 windows was developed. The specific window lists were constructed based on the DDA experiment of the pooled sample. The full scan was set at a resolution of 120,000 over the m/z range of 400 to 900, followed by DIA scans with a resolution of 30,000; the HCD collision energy was 32%, the AGC target was 1E6 and the maximal injection time was 50 ms.

iv) Spectral library generation: To generate a comprehensive spectral library, a pooled sample from each group was processed. DDA data were processed using Proteome Discoverer software (Thermo Fisher Scientific, Inc.) and searched against the human UniProt database (https://sparql.uniprot.org/) appended with the iRT fusion protein sequence (Biognosys AG).

A maximum of two missed cleavages for trypsin were used, cysteine carbamidomethylation was set as a fixed modification, and methionine oxidation deamination and +43 on Kn (Carbamyl) were used as variable modifications. Parent and fragment ion mass tolerances were set to 10 ppm and 0.02 Da, respectively. The applied false discovery rate (FDR) cutoff was 0.01 at the protein level. The results were then imported to Spectronaut Pulsar software (Biognosys AG) to generate the spectral library.

Additionally, DIA data were imported into Spectronaut Pulsar software and searched against the human UniProt database to generate DIA library. The final library was generated by combining DDA and DIA libraries of ccRCC and controls.

v) Data analysis: DIA-MS data were analyzed using Spectronaut Pulsar (Biognosys AG) with default settings. All results were filtered with a Q-value cutoff of 0.01 which corresponded to an FDR of 1%. Proteins identified in more than 50% of the samples in each group were retained for further analysis. Missing values were imputed based on the k-nearest neighbor method. Raw proteomics data were transformed using log2 and then centralized. Wilcoxon signed rank test was implemented with the software R version 4.1.1 (R-project.org).

Table I. Baseline information of enrolled patients from TCGA database and our cohort.

Clinicopathological characteristics	TCGA (n=261)	Our paired sample (n=27)
Survival status		
Alive	217	27
Dead	44	0
Sex		
Male	158	20
Female	103	7
Age	59 (26-90)	57 (24-71)
Laterality		
Left	116	10
Right	145	7
Pathological stage		
G1	13	4
G2	155	19
G3	86	4
G4	7	0
T stage		
T1a	135	13
T1b	105	14
T1	21	0
N stage		
NX	159	0
N0	102	27
Neoadjuvant therapy		
Yes	7	0
No	254	27

TCGA, The Cancer Genome Atlas.

Selection of m6A RNA methylation regulators: After integrating RNA sequencing and proteomic data, 19 m6A RNA methylation regulators were included for further analysis and included: ALKBH5, CBLL1, ELAVL1, FMR1, FTO, FXR2, HNRNPA2B1, HNRNPC, METTL 14, METTL 3, RBM15, RBM15B, RBMX, RBMXL1, WTAP, YTHDC1, YTHDC2, YTHDF2 and YTHDF3.

Uni-variate survival analysis and establishment of prognostic model based on the 19 m6A methylation regulators. To assess the survival impact of every single m6A methylation regulators on early stage ccRCC, univariate survival analysis was applied. Firstly, pROC package (14) was applied to determine the optimal threshold of every single gene expression and then all the ccRCC patients were divided into two subgroups, namely high and low subgroups. Then, Kaplan-Meier survival analysis with log rank test was calculated and displayed with package 'survminer' (15).

Aiming to construct a comprehensive prognostic model, all 19 m6A methylation regulators were included into multivariate Cox's regression analysis with risk scores for each sample being calculated. Prognostic risk scores for ccRCC patients were calculated using the following formula: Risk score=∑ðβi x Exp iÞ, with i representing the number of prognostic m6A expression levels.

According to the median of risk score, all samples were divided into two subgroups: high risk and low risk, and survival curves and time-dependent ROC curves were generated. The Human Protein Atlas (16) was searched to assess the protein expression level of m6A methylation regulators within the prognostic model.

Multivariate Cox analysis and nomogram development for survival predictions. In order to assess the independence of the diagnostic model, certain critical clinical parameters of the patients were included into the multivariate analysis, including sex, age, tumor side, pathological T stage, N stage and tissue grade. Furthermore, these factors were applied using the 'rms' package (17) to develop a survival time nomogram.

Correlations between the prognostic model and tumor infiltrating immune cells. To assess the relationship between

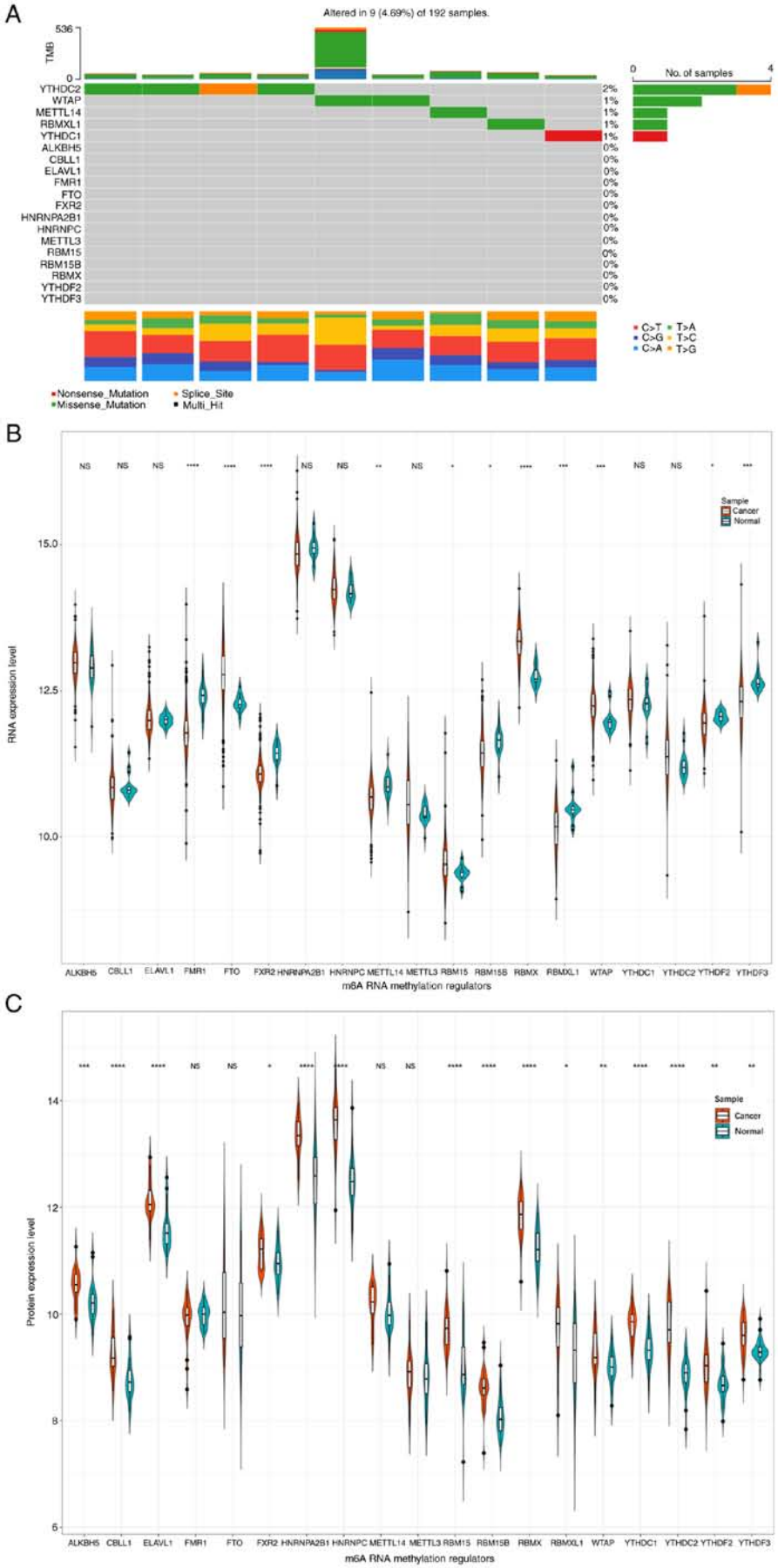

Figure 1. Gene mutation pattern, transcriptome and proteome expression level of m6A methylation regulators in early stage clear cell renal cell carcinoma. (A) The gene mutation pattern of the m6A molecules in the TCGA database. (B) The RNA expression level of the m6A molecules in the TCGA database. (C) The protein expression level in our cohort. *P<0.05, **P<0.01, ***P<0.001 and ****P<0.0001. TCGA, The Cancer Genome Atlas; TMB, tumor mutation burden; NS, not significant.

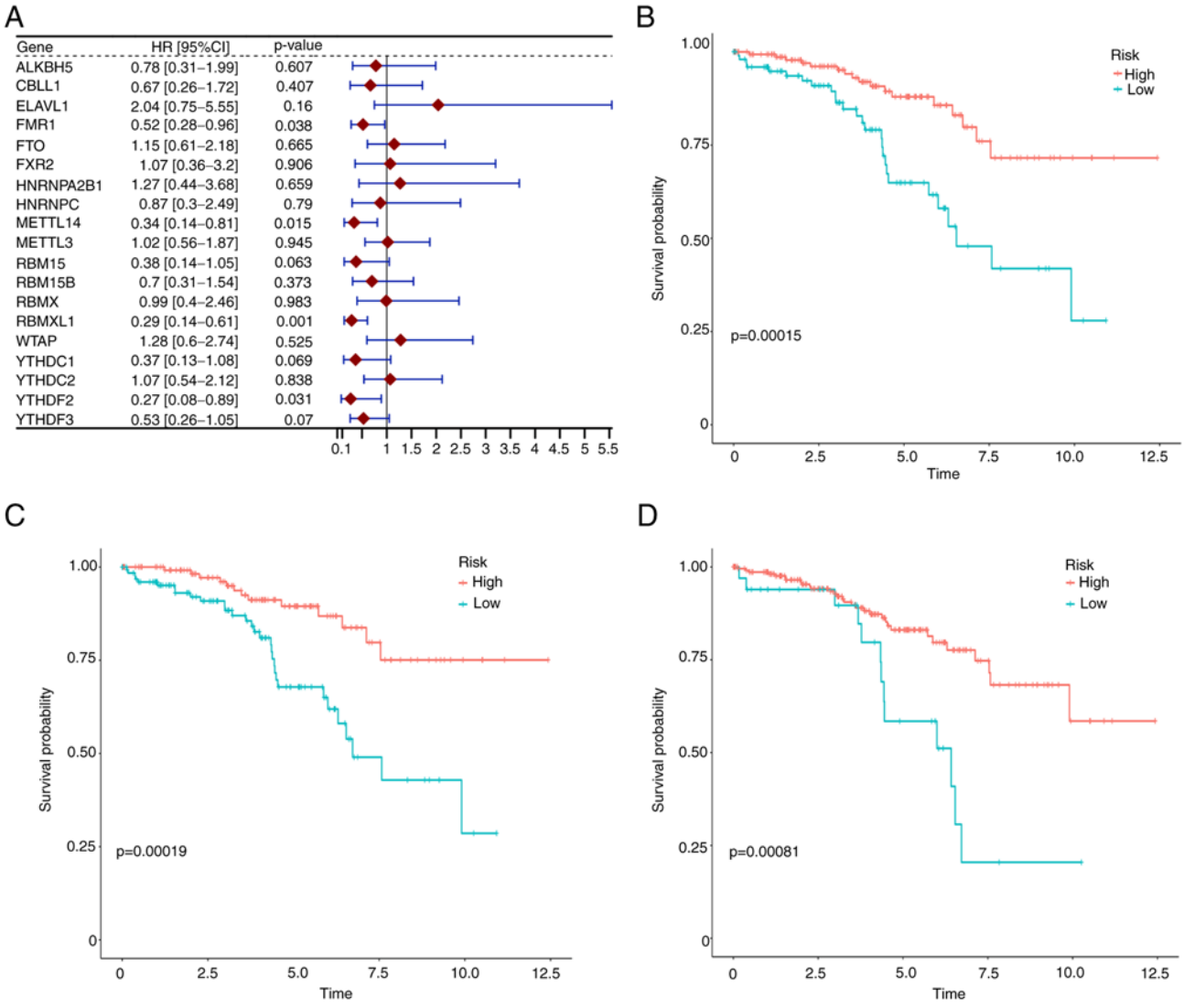

Figure 2. Single variate COX analysis and survival analysis of all the 19 m6A methylation regulators. (A) The forest plot of single variate analysis based on every m6A methylation regulators. (B-D) The survival curves of (B) RBMXL1, (C) YTHDF3 and (D) FMR1.

prognostic model and tumor purity, R package 'estimate' (18) was used to calculate tumor purity, the scores of stromal cells and the infiltration level of immune cells. To further explore the immune cell composition within the tumor microenvironment, Tumor Immune Estimation Resource (TIMER, http://timer.cistrome.org/) was used to compute the proportion of six kinds of immune cells. Spearman's correlation analysis was used to investigate correlations between risk score and immune infiltrating cells. In addition, associations between clinical characteristics, tumor purity and risk scores were analyzed using the standard Kruskal-Wallis test for multi-group (Dunn's test was used for the post hoc analysis) and Wilcoxon signed rank test for two-group comparisons, respectively.

Statistical analysis. All the data analysis and the figures were completed by R (version 4.1.1) as well as corresponding R packages illustrated in the Methods. The non-parametric Spearman's rank correlation analysis was used to calculate the correlation coefficient. All the tests were two-sided, and $P<0.05$ was considered to indicate a statistically significant difference.

Results

Baseline information. Clinical characteristics for 261 TCGA participants and 27 paired proteomic samples have been provided in Table I. At the end of the follow-up period, 44 of 261 patients had succumbed while none of the 27 patients had experienced tumor recurrence or succumbed. The number of men in this cohort was slightly greater than women with a ratio of 158:103 for TCGA and 20:7 in the proteomic sample. In addition, the average age within the two datasets was similar at 59 years for the TCGA group and 57 years for the proteomic sample.

Expression levels of 19 m6A RNA methylation regulators in genome, transcriptome and proteome. Firstly, the gene mutation pattern of the 19 m6A methylation regulator genes was examined (Fig. 1A). It was identified that the mutation frequency was relatively low with a rate of 4.69%. Among the 9 mutated samples, YTHDC2 demonstrated the highest mutation frequency at 2% and was followed by WTAP with 1%. Furthermore, missense mutation was the most common mutation type with a rate of 3.6%.

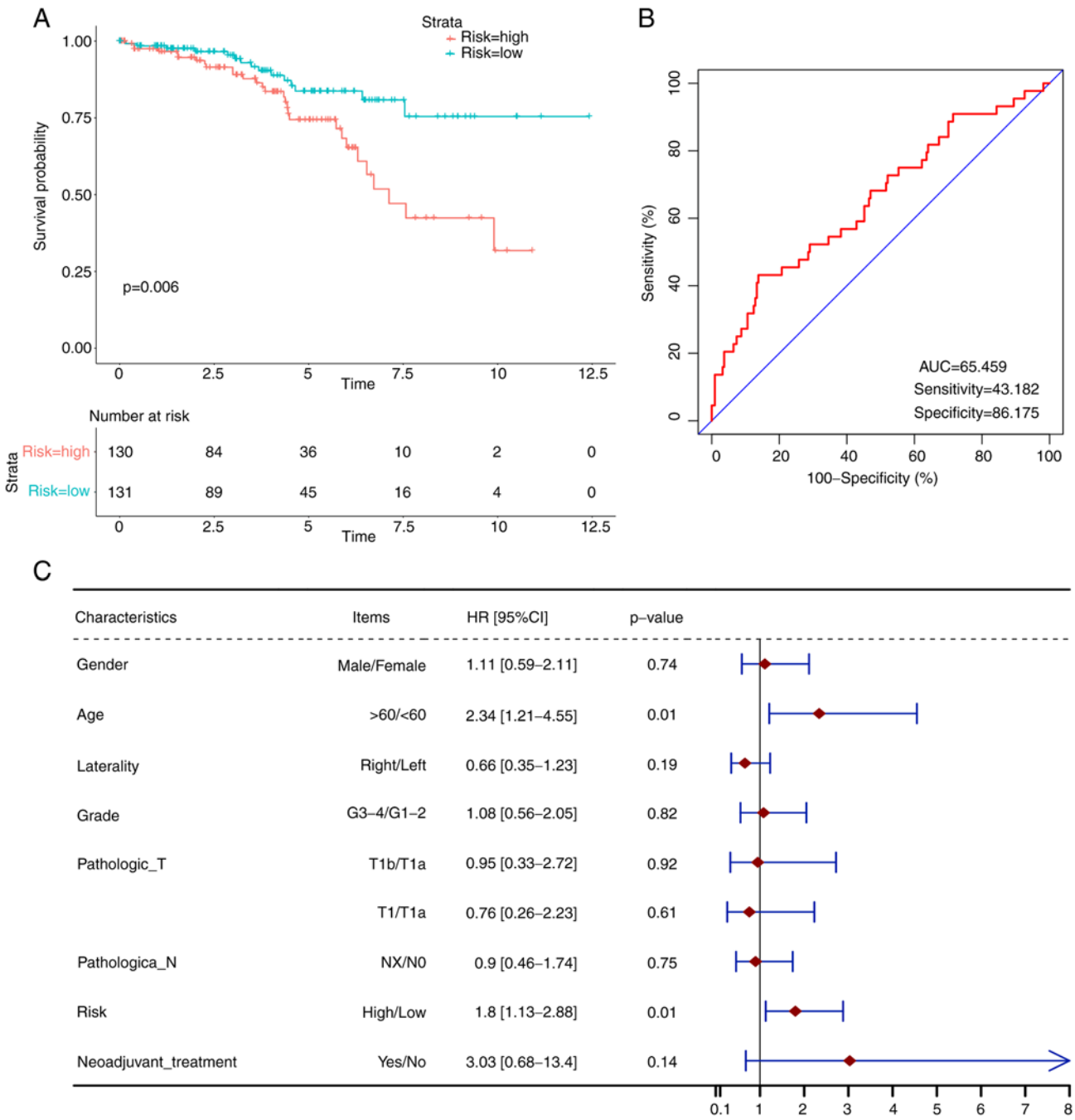

Figure 3. Survival analysis of the m6A methylation regulators based on the prognostic model. (A) The survival curve of the prognostic model. (B) ROC curve of the prognostic model. (C) Forest plot of multi-variate analysis with prognostic model and critical clinical parameters included.

Expression levels for RNA sequencing and proteomic data were presented in Fig. 1B and C, respectively. It was revealed that there existed 11 differentially expressed genes, including 4 upregulated and 7 downregulated m6A regulators (Fig. 1B). According to the level of proteins, 15 aberrantly expressed m6A regulators were detected, except for FMR1, FTO, METTLE14 and METTLE3 (Fig. 1C).

Identification of survival-related m6A methylation regulators. In order to identify survival-related m6A methylation regulators, single-variate Cox analysis was performed and the results were provided in a forest plot (Fig. 2A). It could be clearly observed that the expression of FMR 1, METTL14, RBMXL1 and YTHDF 2 were significantly associated with early-stage ccRCC survival. Notably, all 4 regulators were negatively associated with ccRCC overall survival having hazard ratios (HR) of less than 1. After calculating the best cut-off value of each gene with ROC curves, the survival curves for m6A regulators were plotted. The results suggested that 8 gene expression levels, namely RBMXL1, YTHDF3, FMR1, METTLE14, YTHDF2, ELAVL1, FXR2 and RBM 15 were associated with ccRCC patient survival and the top three are revealed in Fig. 2B-D.

Construction and validation of m6A methylation regulators-based prognostic signature. In order to comprehensively

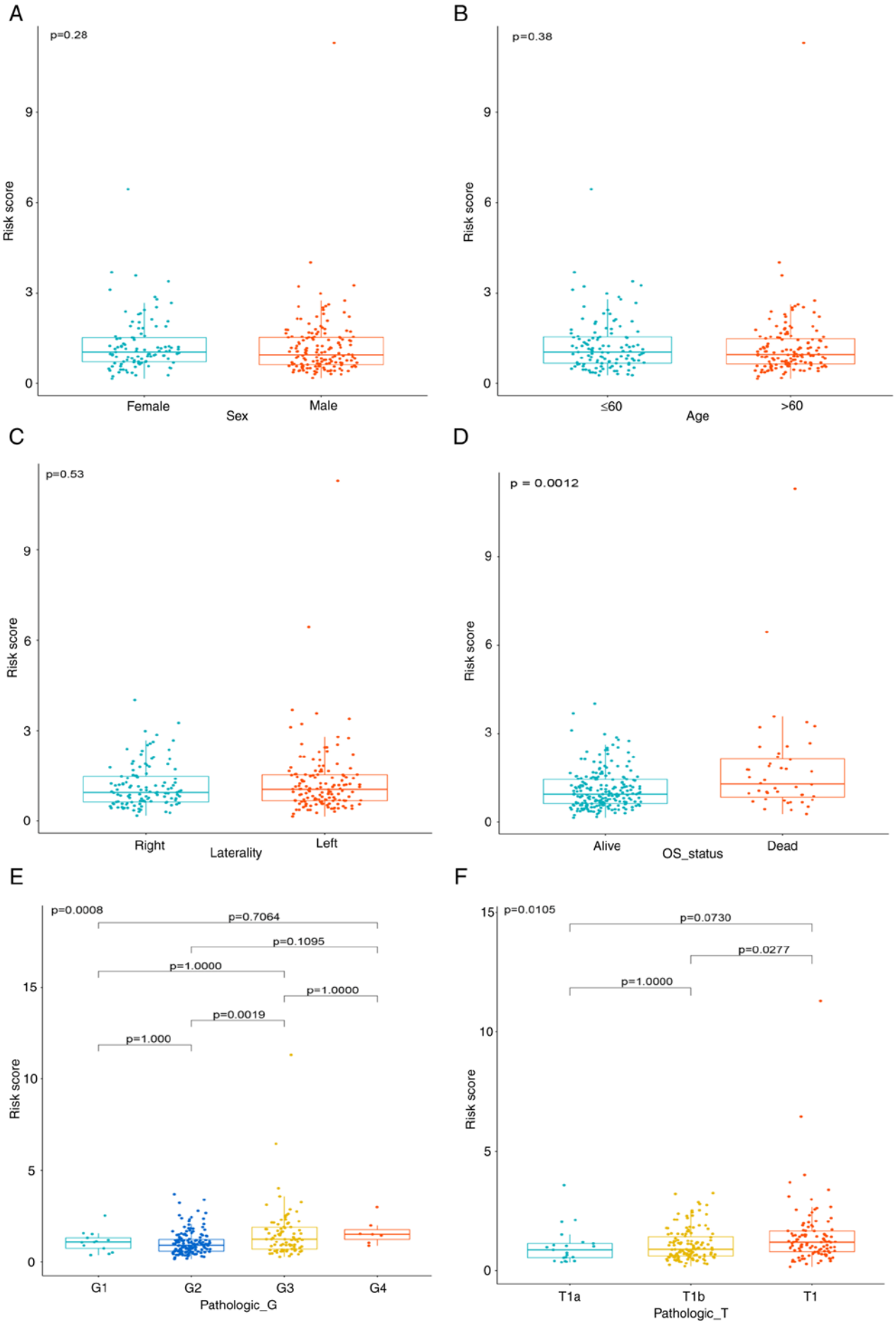

Figure 4. The relationship between risk score and (A) sex, (B) age, (C) tumor site, (D) survival status, (E) pathological grading and (F) pathological T staging.

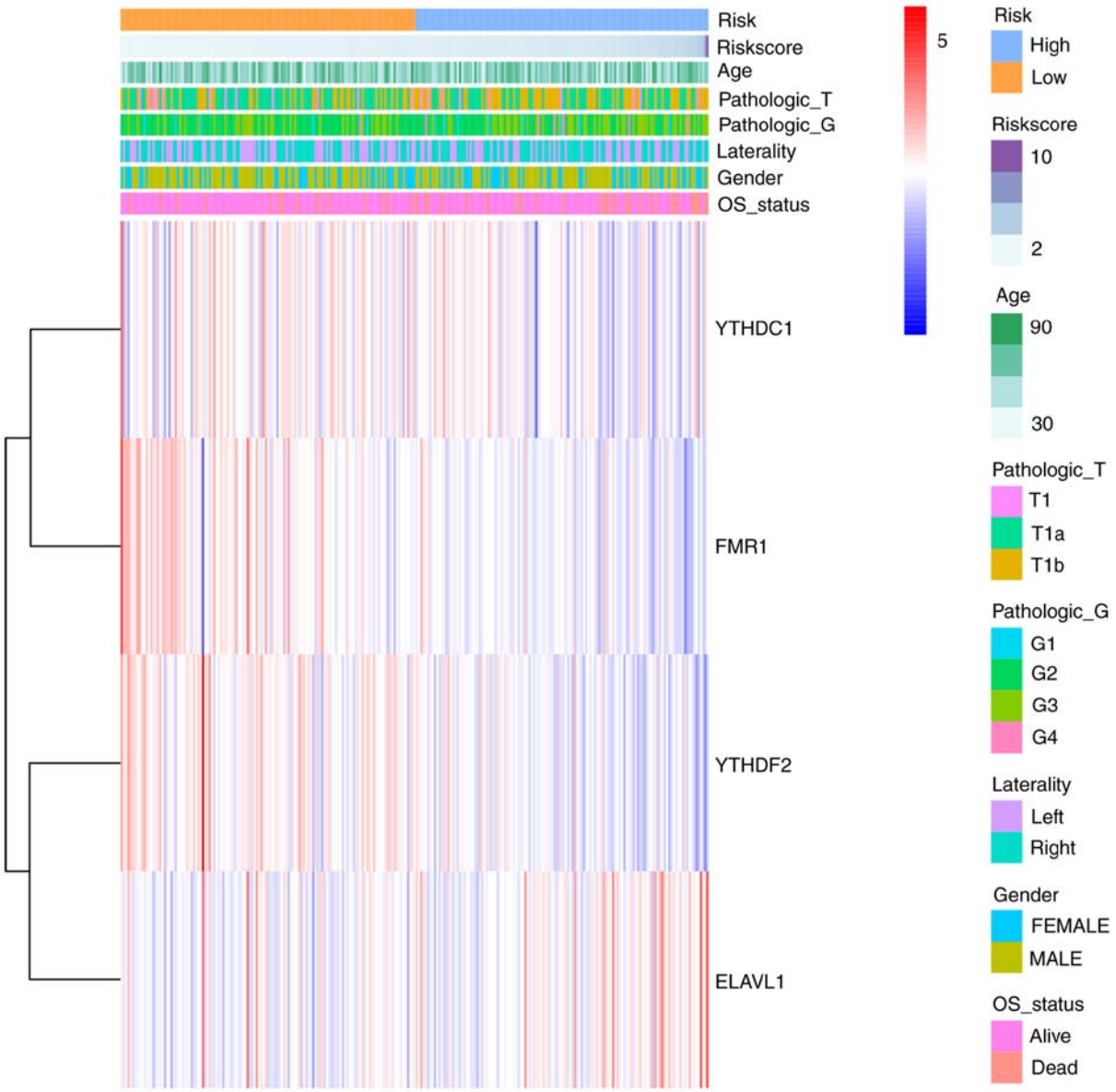

Figure 5. Clustering heat map of the m6A methylation regulators included in the prognostic signature.

describe the predictability of m6A methylation regulators, all 19 m6A regulators were included to construct a prognostic model. After applying multivariate Cox regression analysis, a risk score algorithm was established: Risk score=(-0.54) x expr (YTHDF2) + 0.67 x expr (YTHDC2) + (-1.05) x expr (FMR1) + 1.43 x expr (ELAVL1). Then, all 261 patients were classified into two subgroups according to the median risk score, namely high risk and low risk. Through survival analysis plots, it could be clearly observed that a higher risk score was significantly associated with poorer ccRCC survival (Fig. 3A). To assess the YTHDF2, YTHDC2, FMR1 and ELAVL1 expression, it was found that the immunohistochemistry results from the Human Protein Atlas were in accordance with the risk score. Compared with normal kidney tissue, the expression levels of YTHDF2 and FMR1 within tumor cells were low. In contrast to this situation, the YTHDC2 and ELAVL1 expression levels were upregulated, suggesting the unfavorable role in predicting ccRCC survival (Fig. S1).

To further assess the accuracy of the prognostic model, a ROC curve was generated with an AUC of 65.46% (Fig. 3B). To examine the independency of the model, multivariate Cox analysis with several confirmed critical clinical characteristics was performed and the results showed that the model remained an independent indicator of the survival risk (Fig. 3C).

Furthermore, the association between risk scores and clinical characteristics were also assessed (Fig. 4A-F). The results suggested that risk scores are significantly associated with survival status. A cluster heat map was generated to show RNA expression level for all regulators included in the model (Fig. 5).

Establishing a prognostic nomogram for early-stage ccRCC. To predict survival status more comprehensively and easily, a nomogram was constructed after integrating prognostic risk score and clinical information such as sex, age, laterality, pathological grade, T stage and N stage (Fig. 6). It was revealed that the nomogram is suitable for predicting 1-year, 2-year, 3-year and 5-year survival for ccRCC patients.

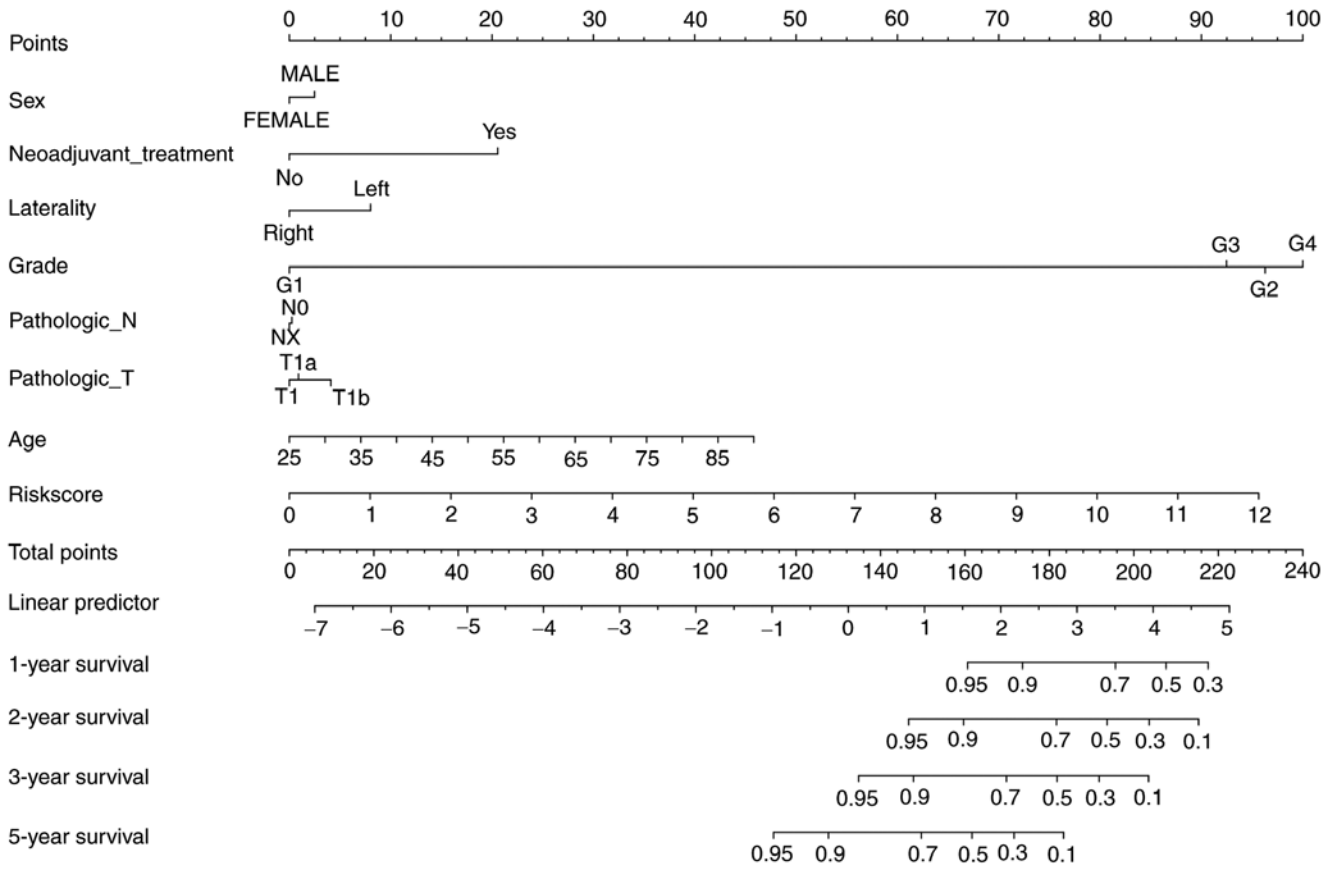

Figure 6. Prognostic nomogram based on the prognostic model and clinical characteristics.

Correlations between risk scores and immune cells in tumor microenvironment. m6A methylation regulators participate in the regulation of tumor microenvironment immune status during tumorigenesis (6). After comparing the tumor purity within different risk subgroups, it was found that the higher risk group was significantly associated with higher immune score ($P<0.001$) and lower tumor purity ($P=0.0066$). However, the stromal score within high and low risk groups did not show significant difference ($P=0.68$) (Fig. 7A-C).

To further confirm which kind of immune cells maybe associated with the prognostic model, Spearman's correlation analysis was implemented to assess the association between risk scores and immune cell composition (Fig. 7D-I). The results revealed that risk scores were statistically associated with various immune cells, including dendritic cells, $CD4^+$ T cells, $CD8^+$ T cells and macrophages as opposed to B cells and neutrophils.

Discussion

As the most common type of renal cancer, the prognosis of ccRCC remains poor with both a high incidence and mortality. Epigenetic modifications, particularly RNA modifications have proven to play various functions in the bioprocess of tumorigenesis and therefore produce a frame of tumor biomarkers (19). This should not be overlooked as a key element in the quest to identify elements which will enable clinicians to identify cases early and to determine those who are more likely to require swift interventions. As the most prevalent type of RNA post-translational modification, m6A has drawn an increasing attention since the identification of the first RNA demethylase in 2011, the fat mass and obesity-associated protein (FTO), revealing that the RNA methylation is a reversible process (20). Numerous studies (21,22) have revealed that FTO is closely related to BMI, which is closely related to the tumorigenesis of ccRCC. But after assessing the relationship between BMI and the proteomic expression of FTO with our cohort, no significant correlation was observed (Fig. S2). Due to the incomplete clinical data of TCGA database, the correlation within the 261 patients was not analyzed, which is a disadvantage of the aforementioned analysis.

In the present study, multi-omics were applied to reveal the prognostic role of m6A methylation regulators in early-stage ccRCC. To the best of our knowledge, the present study is the first one to suggest that m6A could predict the prognosis for pT1 stage ccRCC patients. From the 19 m6A methylation regulators, the expression of four genes were significantly associated with overall survival for ccRCC patients, namely: FMR1, METTL14, RBMXL1 and YTHDF2. To further predict survival, a mode consisting of YTHDF2, YTHDC2, FMR1 and ELAVL1 was constructed based on Cox's regression analysis, which was verified from immunohistochemistry. Additionally, multivariate Cox analysis revealed that the signature was an independent predictor of ccRCC. In order to render our model more applicable, a nomogram that could be more easily adopted into clinical practice was established, although this is also only an initial study. Previous

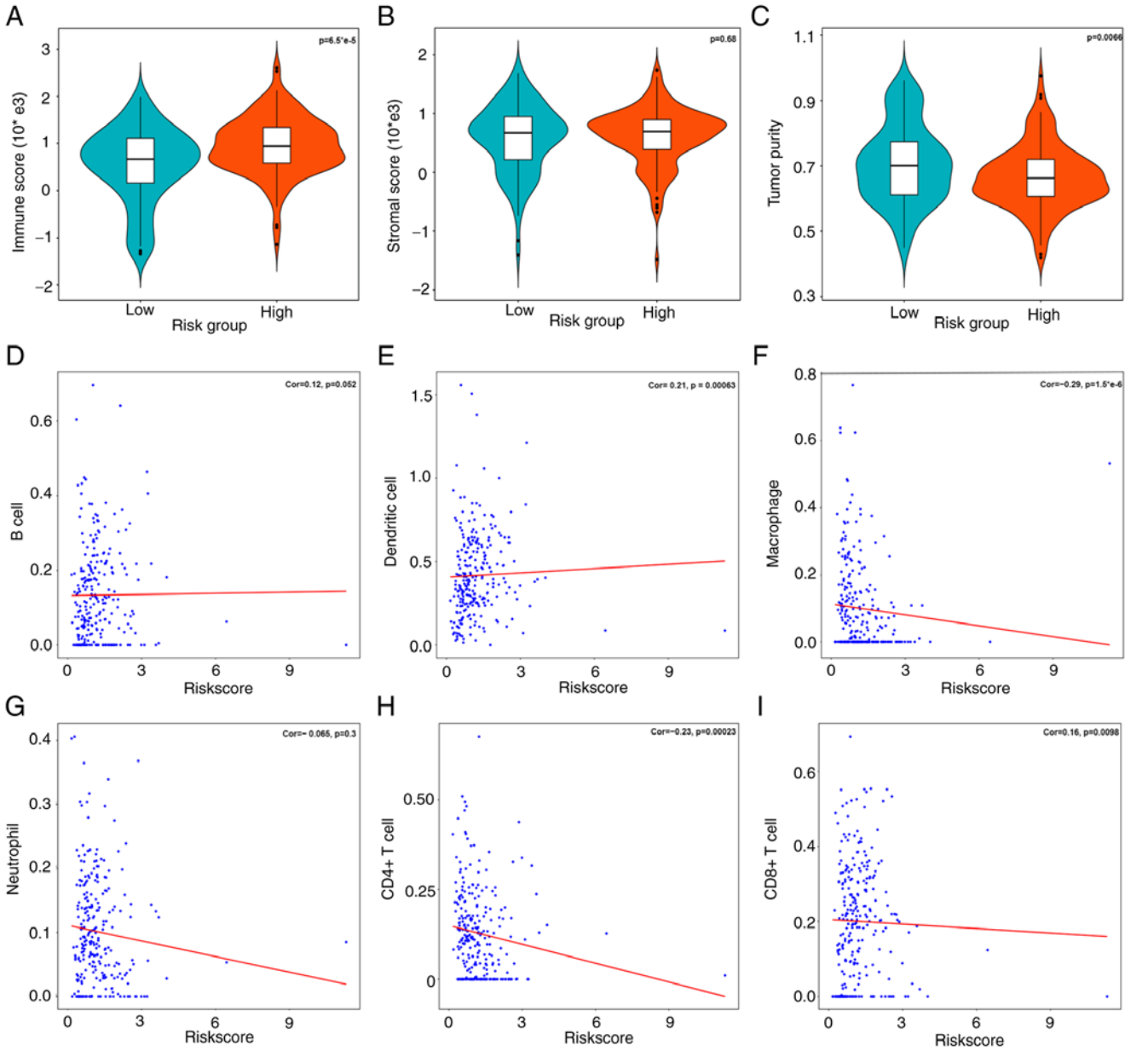

Figure 7. Relationship between prognostic model and the immune cell compositions within the tumor microenvironment. (A-C): The relationship of (A) immune cell scores, (B) stromal cell scores and (C) tumor purity within different risk groups. (D-I): The correlation between immune cell composition with the risk score of the prognostic model using the Spearman's correlation analysis.

studies found that ccRCC is an immune-rich tumor since multiple kinds of immune-infiltrating cells exist in the tumor microenvironment (10,23,24). Therefore, the relationship between the generated prognostic model and immune cells were also assessed with the help of online TIMER software and 'ESTIMATE' package. The results suggested that the m6A methylation prognostic model was significantly associated with dendritic cells, $CD4^+$ T cells, $CD8^+$ T cells and macrophages. This may provide new evidence for the role of m6A methylation in regulating tumor immune-infiltrating microenvironment; however, of course further interdisciplinary research is required.

In our analysis and relative study (25), the molecule YTHDF2 appears to play a critical role since this was not only associated with survival status but also made up a proportion of the prognostic signature. Additionally, protein expression for YTHDF2 between cancer and non-cancerous normal tissues remains differential in the samples examined in the present study. As a member of m6A-binding proteins (i.e. readers), YTHDF2 possesses a YTH binding capability which may interact with m6A modifications for specific RNAs. Therefore, this ability may play a critical role in improving target mRNA translation efficiency (26).

Previous studies have reported that YTHDF2 may participate in the progression of various malignant tumors. For example, Zhang *et al* (27) found that by maintaining m6A methylation of the OCT4 mRNA, YTHDF2 enhances its protein expression and therefore promotes liver cancer stem cell phenotype. This appears to suggest that YTHDF2 acts as an oncogene in the progression of hepatic cell carcinoma (HCC). However conversely, another study has demonstrated that YTHDF2 is a novel tumor suppressor for HCC since it

mechanistically suppresses STAT3 phosphorylation and tumor growth by degrading IL-6 family cytokine-encoded mRNAs (28). Similarly, in glioma studies, YTHDF2 has been found to downregulate the expression of LXRα and HIVEP2 through m6A-dependent mRNA decay and therefore may impact on the survival of glioma patients (29). Xie *et al* (30) revealed that METTL3/YTHDF2 m6A axis may directly degrade mRNAs of tumor suppressors such as SETD7 and KLF4, which can lead to carcinogenesis and progression of bladder cancer.

Another important molecule in the prognostic model is FMR1, which has been found to be involved in the negative regulation of mRNA translation. Recently, the FMR1 was identified as a putative m6A reader which means that it binds to m6A containing transcripts. For example, Edens *et al* (31) showed that FMRP, the protein encoded by FMR1, preferentially binds m6A-modified mRNAs and thereby promotes their nuclear export through CMR1, thus regulating neutral differentiation (32). Notably, FMRP could also bind to m6A sites in targets and interact with YTHDF2, which is yet another 'm6A reader', in an RNA-independent manner. The results suggested that the function of FMR1 was maintaining the stability of its mRNA targets while YTHDF2 focused on the degradation of these transcripts (33).

As an m6A writer, METTL14 mainly performed its function through combining with METTL3 and forming an m6A-METTL complex (MAC). In contrast to the evidenced catalytic function of METTL3, METTL14 appears to be mainly responsible for maintaining MAC integrity and mediating RNA bind (34). Although recently, METTL14 has also been reported to participate in crosstalk between histone modification and RNA methylation. METTL14 thereby could recognize H3K36me3 and facilitate binding between m6A MTC and the adjacent RNA polymerase II, thereby writing m6A into actively transcribed nascent RNAs (35). Zhang *et al* (36) reported that METTL14-mediated m6A modification negatively regulates mRNA stability of bromodomain PHD finger transcription factor, therefore facilitating the tumor metastasis and reprogramming glycolysis of RCC. This suggested that the functions of METTL14-mediated m6A are likely to be multifaceted and demand further research.

Another reader, ELAVL1 also participated in the composition of the prognostic model. Embryonic lethal abnormal visual protein 1 (ELAVL1), known as RNA binding proteins, also called human antigen R (HuR) has been reported to participate in various processes, including nervous system development, cellular proliferation and migration (37). Through binding to specific RNAs, ELAVL1 could increase mRNA stability of target genes. Ronkainen *et al* (38) reported that ELAVL1 was associated with reduced RCC-specific survival and inner mechanism study revealed that the HuR protein could regulate the expression of COX-2 in RCC cells, which maybe a putative mechanism of action for the progression of RCC. In addition, Danilin *et al* (39,40) identified that knockdown of HuR in RCC cell lines could inhibit proliferation and induce apoptosis, the process of which was mediated by inhibiting the PI3K/Akt and MAPK oncogenic signaling pathways. All the evidences suggested that the molecular 'HuR' may be potential drug target for ccRCC.

As a retrospective study, it is necessary to discuss the limitations involved. First, the sample size for the present study was relatively small which inhibits our ability to generalize findings to a broader community. A total of 261 cases with early-stage ccRCC were initially enrolled from the TCGA database and all the subsequent analysis was based on this data. Even though the data is reliable, the sample size remains small for high-throughput omics research. Second, the favorable prognosis, which may be due to a short follow-up period and pathologically pT1 ccRCC, is another shortcoming of the present study. Regarding the survival of enrolled patients from our center, the final event was not found until now since they received the surgery within the period of June 2019 to September 2019. In addition, all the enrolled patients were pT1 ccRCC with pT2 excluded due to the fact that tumorigenesis is a gradual process and pT1 ccRCC may reflect the original status of ccRCC, highlighting the significance of molecular changes of pT1 ccRCC. In the future, our follow-up time will be extended, more patients will be enrolled and the clinical outcomes will be reported to the journal if necessary. To sum up, a larger cohort with much longer follow-up period is required. Third, the lack of external validation of the established prognostic model is also another limitation. GEO dataset, one of the most widely used dataset, has been searched. Nevertheless, it was found that no studies have complete prognostic information as well as RNA sequencing data regarding pT1 ccRCC. Finally, all our analysis was based on the multi-omics data. In order to explore the concrete effect of critical m6A RNA methylation regulators on ccRCC tumorigenesis, more *in vitro* and *in vivo* experiments are required to validate the result in the future.

In conclusion, a prognostic model of early-stage ccRCC with m6A methylation regulators was established. The evidence-based model could predict survival for early stage ccRCC patients and is closely related to various tumor infiltrating immune cells.

Acknowledgements

Not applicable.

Funding

No funding was received.

Availability of data and materials

All data generated or analyzed during this study are included in this published article. To protect the privacy of patients, other information could be only acquired with the permission of the corresponding author.

Authors' contributions

ZW and YuZ designed the study, wrote and revised the manuscript. ZW and MZ performed experiments, data analysis and collection and wrote the manuscript. GZ, WW, YaZ, SS and XW collected data and revised the paper. SS conducted statistical analysis and language editing. All authors have read and approved the final manuscript. ZW and YuZ confirm the authenticity of all the raw data.

Ethics approval and consent to participate

The present study was conducted in accordance with the Declaration of Helsinki and was approved (approval no. KS2021034) by the Institutional Review Board of Peking Union Medical College Hospital, Chinese Academy of Medical Science and Peking Union Medical College (Beijing, China). Formal written consent was provided by all patients.

Patient consent for publication

Not applicable.

Competing interests

The authors declare that they have no competing interests.

References

1. Siegel RL, Miller KD, Fuchs HE and Jemal A: Cancer statistics, 2021. CA Cancer J Clin 71: 7-33, 2021.
2. Capitanio U, Bensalah K, Bex A, Boorjian SA, Bray F, Coleman J, Gore JL, Sun M, Wood C and Russo P: Epidemiology of renal cell carcinoma. Eur Urol 75: 74-84, 2019.
3. Obeng RC, Arnold RS, Ogan K, Master VA, Pattaras JG, Petros JA and Osunkoya AO: Molecular characteristics and markers of advanced clear cell renal cell carcinoma: Pitfalls due to intratumoral heterogeneity and identification of genetic alterations associated with metastasis. Int J Urol 27: 790-797, 2020.
4. Downs TM, Schultzel M, Shi H, Sanders C, Tahir Z and Sadler GR: Renal cell carcinoma: Risk assessment and prognostic factors for newly diagnosed patients. Crit Rev Oncol Hematol 70: 59-70, 2009.
5. Motzer RJ, Jonasch E, Agarwal N, Alva A, Baine M, Beckermann K, Carlo MI, Choueiri TK, Costello BA, Derweesh IA, *et al*: Kidney cancer, version 3.2022, nccn clinical practice guidelines in oncology. J Natl Compr Canc Netw 20: 71-90, 2022.
6. Li N, Kang Y, Wang L, Huff S, Tang R, Hui H, Agrawal K, Gonzalez GM, Wang Y, Patel SP and Rana TM: ALKBH5 regulates anti-PD-1 therapy response by modulating lactate and suppressive immune cell accumulation in tumor microenvironment. Proc Natl Acad Sci USA 117: 20159-20170, 2020.
7. Wu H, Xu Z, Wang Z, Ren Z, Li L and Ruan Y: Exosomes from dendritic cells with Mettl3 gene knockdown prevent immune rejection in a mouse cardiac allograft model. Immunogenetics 72: 423-430, 2020.
8. Wang L, Hui H, Agrawal K, Kang Y, Li N, Tang R, Yuan J and Rana TM: m^{6}A RNA methyltransferases METTL3/14 regulate immune responses to anti-PD-1 therapy. EMBO J 39: e104514, 2020.
9. Liu X, Wang P, Teng X, Zhang Z and Song S: Comprehensive analysis of expression regulation for RNA m6A regulators with clinical significance in human cancers. Front Oncol 11: 624395, 2021.
10. Fang J, Hu M, Sun Y, Zhou S and Li H: Expression profile analysis of m6A RNA methylation regulators indicates they are immune signature associated and can predict survival in kidney renal cell carcinoma. DNA Cell Biol 39: 2194-2211, 2020.
11. Wang J, Zhang C, He W and Gou X: Effect of m^{6}A RNA methylation regulators on malignant progression and prognosis in renal clear cell carcinoma. Front Oncol 10: 3, 2020.
12. Mayakonda A, Lin DC, Assenov Y, Plass C and Koeffler HP: Maftools: Efficient and comprehensive analysis of somatic variants in cancer. Genome Res 28: 1747-1756, 2018.
13. Love MI, Huber W and Anders S: Moderated estimation of fold change and dispersion for RNA-seq data with DESeq2. Genome Biol 15: 550, 2014.
14. Robin X, Turck N, Hainard A, Tiberti N, Lisacek F, Sanchez JC and Müller M: pROC: An open-source package for R and S+ to analyze and compare ROC curves. BMC Bioinformatics 12: 77, 2011.
15. Kassambara A, Kosinski M and Biecek P: Survminer: Drawing survival curves using 'ggplot2'. R package version 0.4.9, 2021. https://CRAN.R-project.org/package=survminer.
16. Uhlén M, Fagerberg L, Hallström BM, Lindskog C, Oksvold P, Mardinoglu A, Sivertsson A, Kampf C, Sjöstedt E, Asplund A, *et al*: Tissue-based map of the human proteome. Science 347: 1260419, 2015.
17. Harrell FE Jr: Rms: Regression modeling strategies. R package version 6.2-0, 2021. https://cran.r-project.org/web/packages/rms/index.html.
18. Yoshihara K, Kim H and Verhaak RG: Estimate: Estimate of stromal and immune cells in malignant tumor tissues from expression data. R package version 1.0.13/r21, 2016. https://r-forge.r-project.org/projects/estimate/.
19. Shen C, Xuan B, Yan T, Ma Y, Xu P, Tian X, Zhang X, Cao Y, Ma D, Zhu X, *et al*: m^{6}A-dependent glycolysis enhances colorectal cancer progression. Mol Cancer 19: 72, 2020.
20. Wang T, Kong S, Tao M and Ju S: The potential role of RNA N6-methyladenosine in cancer progression. Mol Cancer 19: 88, 2020.
21. Wojciechowski P, Lipowska A, Rys P, Ewens KG, Franks S, Tan S, Lerchbaum E, Vcelak J, Attaoua R, Straczkowski M, *et al*: Impact of FTO genotypes on BMI and weight in polycystic ovary syndrome: A systematic review and meta-analysis. Diabetologia 55: 2636-2645, 2012.
22. Zarza-Rebollo JA, Molina E and Rivera M: The role of the FTO gene in the relationship between depression and obesity. A systematic review. Neurosci Biobehav Rev 127: 630-637, 2021.
23. Qiu Y, Wang X, Fan Z, Zhan S, Jiang X and Huang J: Integrated analysis on the N6-methyladenosine-related long noncoding RNAs prognostic signature, immune checkpoints, and immune cell infiltration in clear cell renal cell carcinoma. Immun Inflamm Dis 9: 1596-1612, 2021.
24. Xu T, Gao S, Ruan H, Liu J, Liu Y, Liu D, Tong J, Shi J, Yang H, Chen K and Zhang X: METTL14 Acts as a potential regulator of tumor immune and progression in clear cell renal cell carcinoma. Front Genet 12: 609174, 2021.
25. Mu Z, Dong D, Sun M, Li L, Wei N and Hu B: Prognostic value of YTHDF2 in clear cell renal cell carcinoma. Front Oncol 10: 1566, 2020.
26. Lan Q, Liu PY, Haase J, Bell JL, Hüttelmaier S and Liu T: The critical role of RNA m^{6}A methylation in cancer. Cancer Res 79: 1285-1292, 2019.
27. Zhang C, Huang S, Zhuang H, Ruan S, Zhou Z, Huang K, Ji F, Ma Z, Hou B and He X: YTHDF2 promotes the liver cancer stem cell phenotype and cancer metastasis by regulating OCT4 expression via m6A RNA methylation. Oncogene 39: 4507-4518, 2020.
28. Hou J, Zhang H, Liu J, Zhao Z, Wang J, Lu Z, Hu B, Zhou J, Zhao Z, Feng M, *et al*: YTHDF2 reduction fuels inflammation and vascular abnormalization in hepatocellular carcinoma. Mol Cancer 18: 163, 2019.
29. Fang R, Chen X, Zhang S, Shi H, Ye Y, Shi H, Zou Z, Li P, Guo Q, Ma L, *et al*: EGFR/SRC/ERK-stabilized YTHDF2 promotes cholesterol dysregulation and invasive growth of glioblastoma. Nat Commun 12: 177, 2021.
30. Xie H, Li J, Ying Y, Yan H, Jin K, Ma X, He L, Xu X, Liu B, Wang X, *et al*: METTL3/YTHDF2 m(6)A axis promotes tumorigenesis by degrading SETD7 and KLF4 mRNAs in bladder cancer. J Cell Mol Med 24: 4092-4104, 2020.
31. Edens BM, Vissers C, Su J, Arumugam S, Xu Z, Shi H, Miller N, Ringeling FR, Ming GL, He C and Song H: FMRP modulates neural differentiation through m(6)A-dependent mRNA nuclear export. Cell Rep 28: 845-854.e845, 2019.
32. Hsu PJ, Shi H, Zhu AC, Lu Z, Miller N, Edens BM, Ma YC and He C: The RNA-binding protein FMRP facilitates the nuclear export of N^6-methyladenosine-containing mRNAs. J Biol Chem 294: 19889-19895, 2019.
33. Zhang F, Kang Y, Wang M, Li Y, Xu T, Yang W, Song H, Wu H, Shu Q and Jin P: Fragile X mental retardation protein modulates the stability of its m6A-marked messenger RNA targets. Hum Mol Genet 27: 3936-3950, 2018.
34. Liu L, Wang Y, Wu J, Liu J, Qin Z and Fan H: N^6-Methyladenosine: A potential breakthrough for human cancer. Mol Ther Nucleic Acids 19: 804-813, 2020.
35. Huang H, Weng H, Zhou K, Wu T, Zhao BS, Sun M, Chen Z, Deng X, Xiao G, Auer F, *et al*: Histone H3 trimethylation at lysine 36 guides m^{6}A RNA modification co-transcriptionally. Nature 567: 414-419, 2019.

36. Zhang C, Chen L, Liu Y, Huang J, Liu A, Xu Y, Shen Y, He H and Xu D: Downregulated METTL14 accumulates BPTF that reinforces super-enhancers and distal lung metastasis via glycolytic reprogramming in renal cell carcinoma. Theranostics 11: 3676-3693, 2021.
37. Yang F, Hu A, Li D, Wang J, Guo Y, Liu Y, Li H, Chen Y, Wang X, Huang K, *et al*: Circ-HuR suppresses HuR expression and gastric cancer progression by inhibiting CNBP transactivation. Mol Cancer 18: 158, 2019.
38. Ronkainen H, Vaarala MH, Hirvikoski P and Ristimäki A: HuR expression is a marker of poor prognosis in renal cell carcinoma. Tumour Biol 32: 481-487, 2011.
39. Danilin S, Sourbier C, Thomas L, Rothhut S, Lindner V, Helwig JJ, Jacqmin D, Lang H and Massfelder T: Von hippel-lindau tumor suppressor gene-dependent mRNA stabilization of the survival factor parathyroid hormone-related protein in human renal cell carcinoma by the RNA-binding protein HuR. Carcinogenesis 30: 387-396, 2009.
40. Danilin S, Sourbier C, Thomas L, Lindner V, Rothhut S, Dormoy V, Helwig JJ, Jacqmin D, Lang H and Massfelder T: Role of the RNA-binding protein HuR in human renal cell carcinoma. Carcinogenesis 31: 1018-1026, 2010.